LAWRENCE
LIVERMORE
NATIONAL
LABORATORY

LLNL-JRNL-406720

Relativistic Positron Creation Using Ultra-Intense Short Pulse Lasers

H. Chen, S. Wilks, J. Bonlie, E. Liang, J. Myatt, D. Price, D. Meyerhofer, P. Beiersdorfer

September 3, 2008

Physical Review Letters

Disclaimer

Relativistic Positron Creation Using Ultra-Intense Short Pulse Lasers

Hui Chen[1], Scott C. Wilks[1], James D. Bonlie[1], Edison P. Liang[2], Jason Myatt[3], Dwight F. Price[1], David D. Meyerhofer[3], and Peter Beiersdorfer[1]

[1]*Lawrence Livermore National Laboratory, Livermore, CA 94550*

[2]*Rice University, Houston, TX 77005 and*

[3]*University of Rochester, Rochester, NY 14623*

(Dated: September 14, 2008)

Abstract

We measure up to 2×10^{10} positrons per steradian ejected out the back of ∼mm thick gold targets when illuminated with short (∼1 ps) ultra-intense ($\sim1\times10^{20}$ W/cm^2) laser pulses. Positrons produced predominately by the Bethe-Heitler process and have an effective temperature of 2 – 4 MeV, with the distribution peaking at 4 – 7 MeV. The angular distribution of the positrons is anisotropic. The measurements indicate the laser produced, relativistic positron densities ($\sim10^{16}$ positrons/cm^3) are the highest ever created in the laboratory.

PACS numbers: 52.38.-r, 52.38.Ph, 52.59.-f

The ability to create large numbers of MeV positrons in the laboratory opens the door to multiple new avenues of antimatter research, including an understanding of the physics underlying various astrophysical phenomena such as black holes and gamma ray bursts [1, 2], basic pair plasma physics [3, 4], positronium production and positronium Bose-Einstein condensates [5–7]. The use of short, ultra-intense, laser pulses represents a promising new approach to achieve this, given the rapid increase in available energy and intensity of laser systems. Since first theorized in 1973 [8], the use of ultra-intense lasers to generate positrons has been studied in great detail through theory and modeling [2, 9–14]. It has been predicted that for thick high-Z targets, positron generation through the Bethe-Heitler (BH) process [15] is dominates over that from the electron-ion collisions (Trident process [15]) [11, 12]. For thin targets (less than 30 microns for solid gold) the reverse is expected [2]. In the BH process, the laser produced hot electrons make the high energy bremsstrahlung photons that produce electron-positron pairs interacting with the nuclei, while in the Trident process the hot electrons produce pairs directly interacting with the nuclei. Although estimates vary, approximately 10^{10} to 10^{11} positrons/kJ of laser energy are predicted to be created, assuming various laser target conditions [12–14]. Experimentally, the ability of intense short laser pulses to create positrons in laser-solid interaction was first demonstrated on the Nova peta-watt laser by Cowan *et al.* [16] and later on a tabletop laser by Gahn *et al.* [17], where small numbers of positrons were measured.

In this Letter, up to 2×10^{10} positrons/sr with positron kinetic energy up to 20 MeV were observed by irradiating ∼millimeter thick gold targets with short pulse lasers. For the first time positron temperatures were measured, and they were found to be about half that of hot electron temperature. A strong anisotropy in the angular positron emission was observed, with the number ejected in the laser forward direction being more than 10 times the number in the backwards direction on a given shot. The positron density inside the target is estimated to be about 10^{16} positrons/cm^3, making this the densest positron plasma achieved in the laboratory. These conclusions result from the highest statistics and energy resolution positron spectra ever obtained using short pulse lasers. The data are consistent with the BH process in which positrons were produced by MeV photons interacting with gold nuclei.

The experiment was carried out at the two-beam Titan laser at the Jupiter laser facility [18] at Lawrence Livermore National Laboratory. For the experiments described here, the

pulse-length of the short pulse laser (1054 nm, p-polarized) was varied between 0.7 ps to 10 ps, and the laser energy was between 120 J to 250 J. Focused with an $f/3$ off-axis parabola, the full-width at half-maximum of the focal spot was about 8 microns contains about 60% of laser energy. In addition, a 150 J, 3 ns long-pulse laser, at 2ω (527 nm), was fired 4 – 6 ns earlier than the short-pulse laser to produce a large preformed plasma in some shots. The spot diameter of the long-pulse beam was 600 micron using a continuous phase plate [19]. The short pulse laser spot was aligned to the center of the long-pulse laser spot. The experimental setup is shown in Fig. 1. The short pulse was incident to the targets at an 18-degree angle while long-pulse was incident at a 45-degree angle to target normal. Two absolutely calibrated electron-positron spectrometers [20] observed the hot electrons and the positrons from the targets with energy coverage from 0.1 – 100 MeV and a resolution E/δE of 10 – 100. The energy coverage and resolution are higher that was previous achieved in positron energy measurement [16, 17], where positrons were measured at one [17] or several energy points [16]. The absolute calibration was made using electrons [21]. Because there is little difference ($\sim$ 2 – 3%) in positron and electron stopping in the detector materials [22], the electron calibration is applicable to the positrons. The solid angle for the forward spectrometer is 8.2×10^{-5} steradian and 4.5×10^{-5} steradian for the backwards-spectrometer. The targets were disks of solid gold (Z=79), tantalum (Z=73), copper (Z=29), tin (Z=50), and aluminum (Z=13) with 6.38 mm diameter and thicknesses between 0.1 to 3.1 mm.

The peak short-pulse laser intensity ranged from 3×10^{19} to 2×10^{20} W/cm^2. The effective hot electron temperatures for electrons with energies between 5 MeV and the maximum ($\sim$60 MeV) were 3.2 to 9.4 MeV, which were about 2 to 4 times higher than that predicted by the ponderomotive scaling [23]. This is attributed to laser wake-field like accelerated electrons in the large preformed plasma that substantially enhances the predicted temperature scaling. The long-pulse created preformed plasma increased the hot electron temperature and number by 20 – 30%. The scale-length of the preformed plasma was estimated to be approximately 100 microns according to rad-hydro simulations [24]. The difference from ponderomotive scaling is more pronounced when the short-pulse pulse length is longer. The number of hot electrons above 2 MeV (which are relevant to the creation of positrons) was 2.5×10^{11}/sr to 1.4×10^{12}/sr.

Positron signals from Au and Ta targets were observed once the thickness exceeded 250 microns. Figure 2 shows the raw data image for a 1 mm Au target and the lineout through

the signal and background. The background was mainly caused by high-energy photons passing through the housing of the spectrometer into the detector. Those photons were both directly from the target and from secondary radiation around the target chamber. The background evenly illuminates the detector beyond the slit, and therefore it is easily subtracted from the signal, which came only from the collimator and slit of the spectrometer. The signal was verified to be from positrons using methods such as differentiating particles using mass stopping by adding plastic foils, and shooting lower-Z targets, such as Al, Cu, and Sn for the same laser conditions as for shooting Au targets. While the hot electron production for those lower-Z targets was similar to that from Au, there was no positron signal above the background. The absence of signal was consistent with the Z^4 scaling of the BH positron yield that would result in more than an order of magnitude fewer positrons in these lower-Z targets [12]. For thinner (0.1 to 0.25 mm) Au targets, positrons were not observed above the background. This is because fewer pairs would be produced from thinner targets [12] due to the reduced interaction range between photons and electrons with Au nuclei. Thinner targets have more high-energy photon yield [25] contributing to a higher background and therefore a higher positron detection threshold.

The yield of positrons was determined by scaling the positrons to the number of hot electrons that were detected. Figure 3 shows the electron spectrum from the forward spectrometer and the positron spectra from both the forward and backward spectrometers for a 126 J, 2 ps short-pulse shot without a long-pulse. The electron spectrum from the backward spectrometer is similar to that of the forward spectrometer and is not included. The detection limit is about 1×10^8/MeV/sr for the forward spectrometer and about 2×10^7/MeV/sr for the backward spectrometer. The higher energy section (5 – 45 MeV) of the electron spectrum is more relevant to positron creation, and it had a temperature of 4.8±0.4 MeV and an electron number of about 7×10^{11}/sr. The positron numbers are about 1.6×10^{10}/sr from forward spectrometer and 2×10^9/sr from the backward spectrometer. The peaks of both positron spectra are at about 6 MeV, and the effective positron temperature is 2.8±0.3 MeV. This first experimental positron temperature measurement enabled the electron and positron temperatures to be compared: the measured positron temperature was found to be approximately half that of the effective electron temperature. This may be explained as follows: an electron (via a photon) in the original electron spectra is, in effect, splitting its energy into the newly created positron and electron. Therefore one would expect the positron to

be half as energetic as the source electron.

A striking difference is shown in the number of positrons from the forward and backwards direction (Fig. 3 (a)). This is the first observation of an anisotropic distribution of the laser-generated positrons. Ten times more positrons were observed from the laser propagation direction than the backwards direction.

While the inferred hot electron numbers for the Nova peta-watt experiment [16] were similar to that measured in this experiment, more than two orders of magnitude more positrons were observed in the forward direction from the present experiment than that on Nova peta-watt experiment, where the positrons were measured at the forward direction, 30-degree from the laser axis [16]. This may be due to the preformed plasma conditions, and target thickness ($\sim$1 mm verse 0.125 mm in Nova PW), and possibly a sub-optimal observation angle used in Nova that were different from this experiment.

Calculations using the measured hot electron temperature with the given target parameters show that the MeV x-ray bremsstrahlung photons (BH process) process dominates in the positron production processes in thick targets. The ratio of positrons generated by the BH verses Trident processes is $\mathrm{N}_{BH}/\mathrm{N}_{Trident} \sim 400$ for 1 mm thick Au (compared to about 4 for a 0.1 mm Au target.) The positron temperature (the slope of the energy spectrum) can be estimated from a simple formula $d\mathrm{N}_{e+}/d\mathrm{E}_{e+}=\int_E f(\mathrm{E})\sigma_{BH}(\mathrm{E},\mathrm{E}_{e+})d\mathrm{E}$, where $f(\mathrm{E})$ is the bremsstrahlung photon energy distribution, and σ is the positron creation differential cross section [15]. Approximating the bremsstrahlung temperature to be that of the measured hot electrons, an effective temperature for the positrons of about half that of the electrons is obtained, as shown in Fig. 3 (b). This is consistent with the experimental data (Fig. 3 (a)). The positron spectrum obtained from the above calculation is for all positrons generated inside the target. To model the emergent positron spectrum measured by the spectrometer, one has to fold in the positron transport inside the target. This was accomplished by a Monte Carlo code EGSnrc [26]. This code includes only BH pair production and is well suited for our thick target cases. In addition to calculating the positron generation, it self-consistently treats the attenuation effects of the electrons, photons, and positrons as they propagate through a cold solid target. The measured hot electron temperature shown in Fig. 3 (b) is used as the starting distribution of hot electrons. The positron spectra outside the target were modeled at the same angular positions relative to the target as in the experiment. The simulated positron spectra agree not only with the positron temperature

(slope of the spectrum) seen in the experiment, but also with the relative positron number. We note that the peak of positrons from the simulation is at about 2 MeV (as in a previous prediction [12]), rather than at the measured ∼6 MeV. This discrepancy may be due to the fact that neither the analytic formula nor EGS simulations include plasma effects. For example, a sheath electric field may have accelerated the positrons as they left the target, similar to the target normal sheath acceleration field (typically of order of several MeV) for protons [27]. This is supported by the fact that protons with energies of 1 – 4 MeV were observed for the shot shown in Fig. 3 and the same sheath field that accelerates the protons would certainly influence the positron spectrum.

The yield of positrons increases as a function of hot electron temperature (i.e. laser intensity) for a given target thickness, as predicted theoretically [12, 14]. The yield of positrons also increases as a function of target thickness, as shown Fig. 4. Theoretically, the increase of positron yield with target thickness has been shown for thinner targets by Nakashima and Takabe [12]. For a thick target (2 mm lead), Gahn *et al.* [28] calculated that for an electron kinetic energy above 5 – 15 MeV, the positron yield is between 5×10^{-3} and 4×10^{-2}, comparable to our measured yield of about 2×10^{-2}. Figure 4 shows the results from the analytical model and simulation using EGS for these experimental conditions. In the analytic model, the yield was estimated using the BH pair creation process combined with positron and electron attenuation inside the target, indicating that the positron yield per hot electron detected increases as target thickness, until the target thickness is greater than about 5 – 6 mm. Although there is a general qualitative agreement between theory/modeling and experiments, both the analytic model and the EGS simulation underestimate the positron yield for thickness less than 1 mm. This difference may again be due to differences in angular distributions of positrons versus electrons and complex plasma effects, such as electron/positron transport and the electromagnetic field, lacking in the theory and EGS modeling.

The forward spectrometer data corresponds to 2×10^{10} observed positrons/sr for about 120 J laser energy for 1 mm target. From the EGS simulations, at least a factor of 10 more positrons is expected to be trapped inside the target. Given the bremsstrahlung photon and target interaction volume determined from the simulation to be approximately 2×10^{-5} cm^3, the positron density in the target is estimated to be about 1×10^{16} positrons/cm^3, which is the highest MeV positron density ever created in the laboratory, albeit in the presence of gold atoms at solid density. If all of the positrons are created in the order of ∼ps, then the rate

of positron production is of the order of 2×10^{22}/s/sr. Since the number of positrons scales with energy, 10 times this rate is expected from a kJ class short pulse laser like OMEGA EP laser [29] and even higher numbers with lasers such as NIF-ARC [30].

These results potentially enable many important applications of the laser-produced intense positron sources. For example, the understanding of many astrophysical phenomena, from pulsar winds to gamma ray bursts, hinges on the understanding of pair-dominated and hybrid pair-electron-ion plasmas. Another important application of the intense positron source is the formation of high-density positronium (Ps) gas. Due to its short lifetime (0.14 msec for ortho-Ps, 0.1 ns for para-Ps) current Ps densities achievable in the laboratory [31] are strongly limited by the positron flux available to create Ps ($<10^9$ e+/s). Since our laser-produced positron flux is at least 10 orders of magnitude higher, a completely new regime is now, in principle, accessible to Ps physics. Finally, to achieve a Bose-Einstein condensate (BEC) at liquid helium temperature, the Ps density needed is about 4×10^{17} cm^{-3} [7], which is only a factor of $\sim$40 higher than the positron density reported in this Letter. Even though the conversion efficiency of MeV positrons to slow positrons and then to Ps would be much less than unity, given the observed favorable scaling of positron yield with increasing target thickness and laser energy, it is optimistic that a BEC of Ps might be achievable with higher energy ultra-intense lasers in the near future.

Acknowledgments

This work was performed under the auspices of the U.S. Department of Energy by Lawrence Livermore National Laboratory under Contract DE-AC52-07NA27344 and was funded by LDRD-08-LW-058. Work performed by the University of Rochester was supported by the U.S. D.O.E Office of Inertial Confinement Fusion under Cooperative Agreement No. DE-FC52-08NA28302, the University of Rochester, and the New York State Energy Research and Development Authority. We gratefully acknowledge support from the staff at Jupiter Laser Facility and Drs. Mark Eckart, William Craig and William Goldstein, and discussions with Drs. Robert Heeter, Marilyn Schneider and Ronnie Shepherd.

[1] B. A. Remington *et al.*, Science **248**, 1488 (1999).

[2] E. P. Liang, S. C. Wilks, and M. Tabak, Phys. Rev. Lett. **81**, 4887 (1998).

[3] H. A. Weldon, Phys. Rev. Lett. **66**, 293, (1991).

[4] E. G. Blackman and G. B. Field, Phys. Rev. Lett. **71**, 3481, (1993).

[5] P. M. Platzman and A. P. Mills Jr. Phys. Rev. B. **49**, 454 (1994).

[6] A. P. Mills Jr., Nucl. Instrum. and Methods in Phys. Research Sec. B, 192, 107, (2002)

[7] E. P. Liang and C. D. Dermer, Opt. Comm. **65**, 419 (1988).

[8] J. W. Shearer *et al.*, Phys. Rev. A **8**, 1582 (1973).

[9] B. Shen and J. Meyer-ter-Vehn, Phys. Rev. E. **65**, 016405 (2001).

[10] P. L. Shkolnikov *et al.*, Appl. Phys. Lett. **71**, 3471 (1997).

[11] D. A. Gryaznykh Y. Z. Kandiev, and V. A. Lykov, JETP Lett. **67**, 257 (1998).

[12] K. Nakashima and H. Takabe, Phys. Plasmas **9**, 1505 (2002).

[13] V.I. Berezhiani, D.P. Garuchava and P.K. Shukla, Physics Letters A **360**, 624 (2007).

[14] J. Myatt *et al.*, sumbitted to PRE. (2008).

[15] W. Heitler, The Quantum Theory of Radiation (Clarendon Press, Oxford, 1954)

[16] T. E. Cowan *et al.*, Laser Part. Beams **17**, 773 (1999).

[17] C. Gahn *et al.*, Applied Physics Letters **77**, 2662 (2000).

[18] http://jlf.llnl.gov

[19] S. N. Dixit *et al.*, Optical Letters **21**, 1715 (1996).

[20] H. Chen *et al.*, Rev. Sci. Instrum. **79**, 1 (2008).

[21] H. Chen *et al.*, REV. SCI. INSTRUM. **79**, 033301 (2008).

[22] F. Rohrlich and B. C. Carlson, Phys. Rev. **93**, 38 (1954).

[23] S. C. Wilks *et al.*, Phys. Rev. Lett. **69**, 1383 (1992).

[24] M. Marinak *et al.*, Phys. Rev. Lett. **75**, 3677 (1995)

[25] S. P. Hatchett *et al.*, Phys. Plasmas **7**, 2076 (2000).

[26] I. Kawrakow and D. W. O. Rogers, National Research Council of Canada Report PIRS-701 (2006).

[27] S. C. Wilks *et al.*, Physics of Plasmas **8**, 542 (2001).

[28] C. Gahn *et al.*, Physics of Plasmas **9**, 987 (2002).

[29] L. J. Waxter *et al.*, Opt. Photonics News **16**, 30 (2005).

[30] M. H. Key, Phys. Plasmas **14**, 055502 (2007).

[31] C. M. Surko and R. G. Greaves, Physics of Plasmas **11**, 2333 (2004).

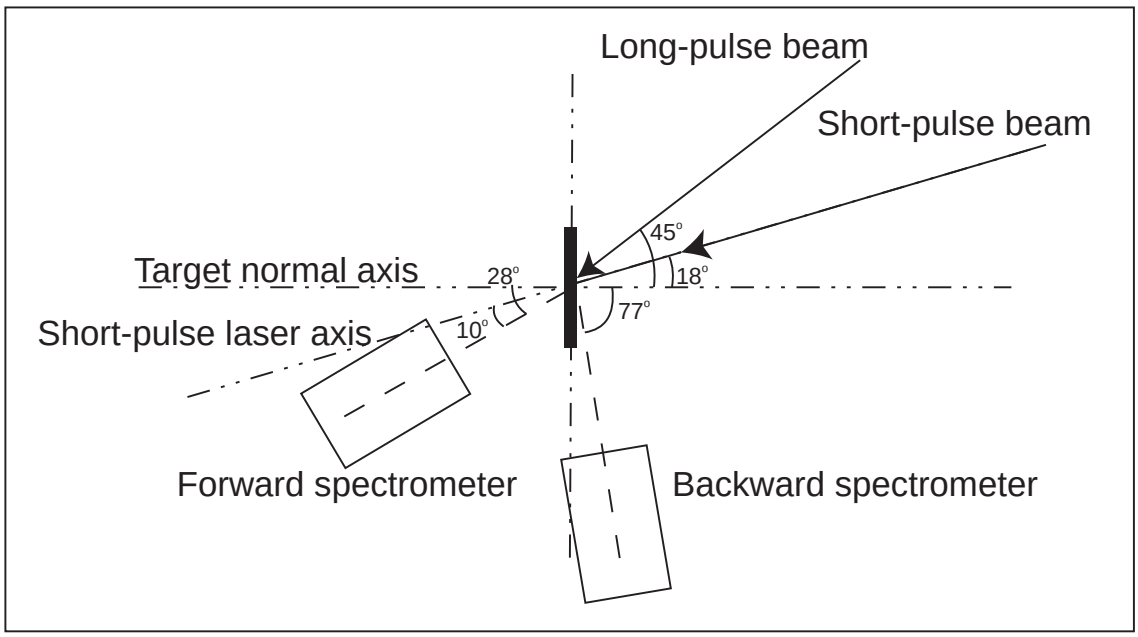

FIG. 1: Illustration of the experimental set up. The two spectrometer positrons relative to the lasers and target are marked.

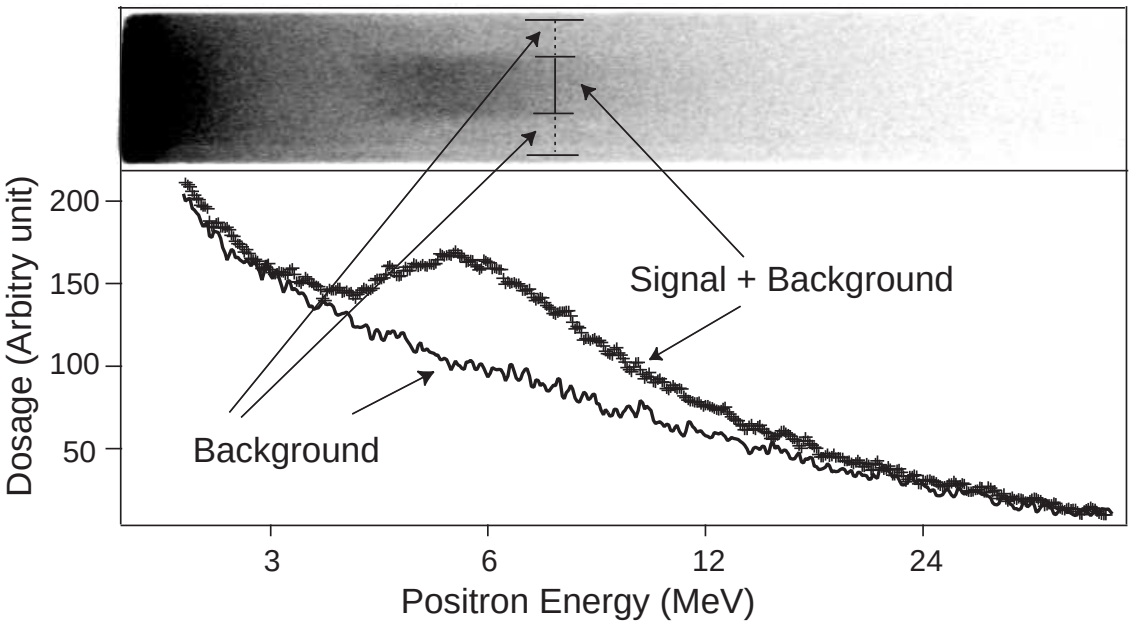

FIG. 2: Raw positron data image and lineouts. This shot had 139 J of short-pulse laser energy with a pulse duration of 0.7 ps. The long-pulse laser energy was 128 J with a 3 ns pulse duration. The long-pulse fired 4 ns before the short-pulse beam. The target thickness was 1 mm.

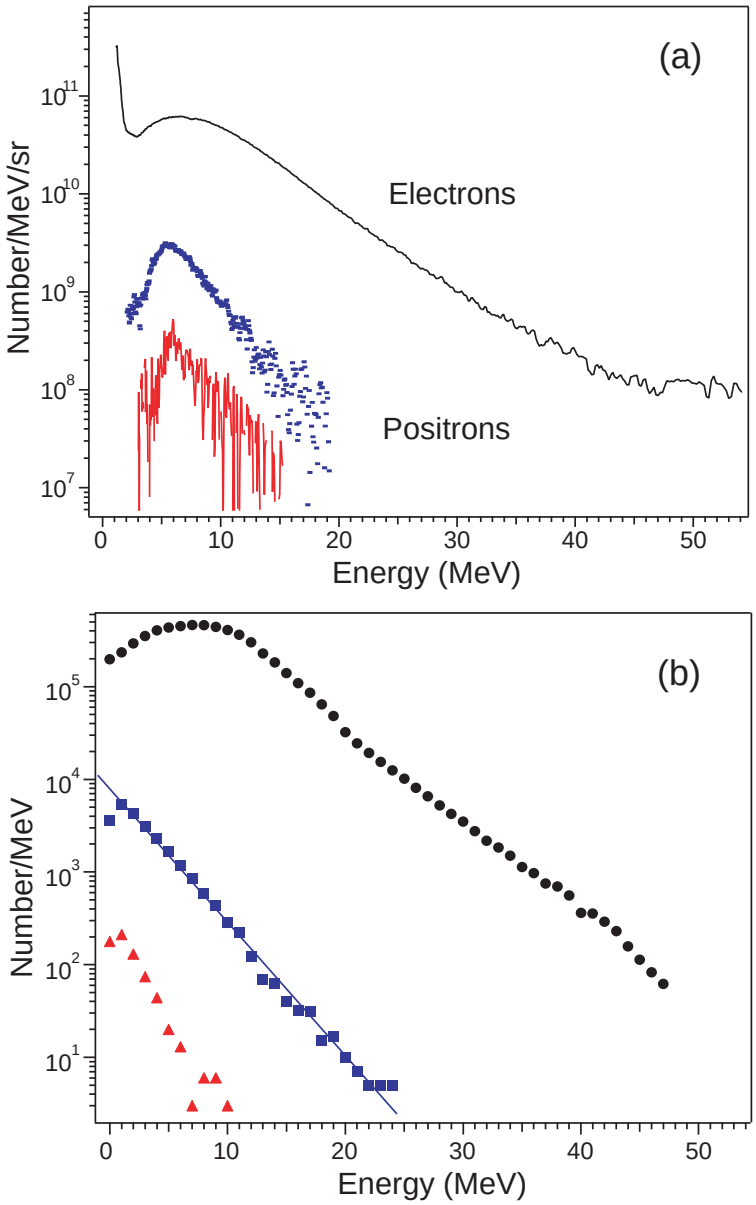

FIG. 3: Energy spectra of electrons and positrons from experiments (a) and EGS modeling (b). On both (a) and (b), the electron spectrum is at the top and the two positron spectra are at the bottom. The positron spectrum from the back of the target has the higher number of counts of the two. The solid line in (b) is the slope from the analytic formula.

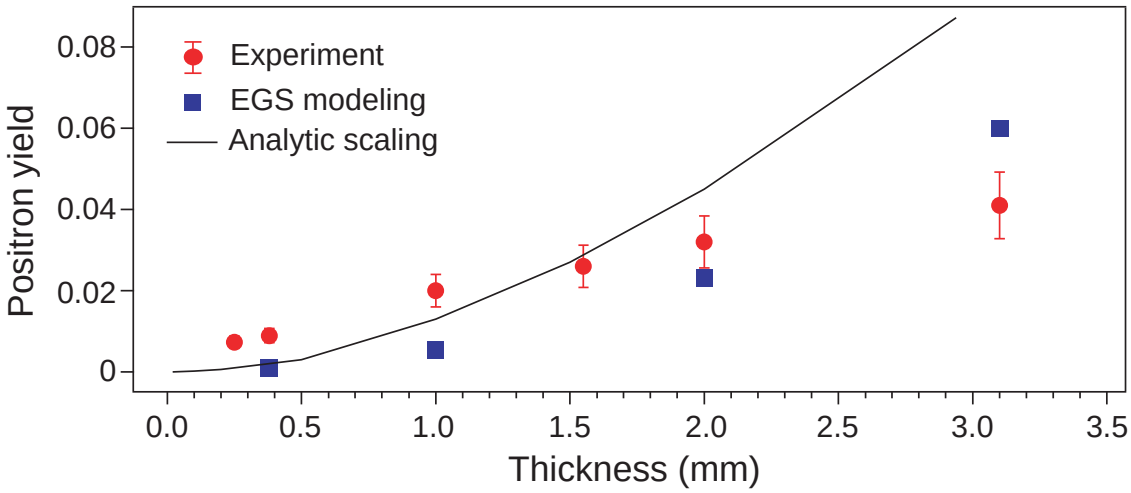

FIG. 4: Positron yield per hot electron as a function of Au target thickness. The short-pulse duration was 0.7 ps for all data points. The laser intensities were from 1.5 – 1.8 $\times 10^{20}$ W/cm^2, hot electron temperature from 5.5 – 7 MeV.